Photofission and total photoabsorption cross sections in the energy range of shadowing effects

A. Deppman,[1] G. Silva,[1] S. Anefalos,[1] S. B. Duarte,[2] F. García,[1,3] F. H. Hisamoto,[1] and O. A. P. Tavares[2]
[1]*Instituto de Física, Universidade de São Paulo, CP 66318, CEP 05315-970, São Paulo, Brazil*
[2]*Centro Brasileiro de Pesquisas Físicas, CBPF/MCT, CEP 22290-180, Rio de Janeiro, Brazil*
[3]*Universidade Estadual de Santa Cruz, UESC, CEP 45650-000, Ilhéus, Brazil*
(Received 30 January 2006; published 28 June 2006)

The energy dependence of photofission cross section for heavy nuclei has recently been well described in terms of a Monte Carlo calculation at energies from the pion photoproduction threshold up to 1 GeV [see, for instance, A. Deppman *et al*., Phys. Rev. Lett. **87** (2001) 182701]. Recent experimental data from CLAS (CEBAF Large Angle Spectrometer) collaboration have extended the measured photofission cross section up to 3.5 GeV for actinide and preactinide nuclei. In this work we address the calculation of photoabsorption and photofission cross sections for actinide and preactinide nuclei above 1 GeV, a region where the shadowing effect plays an important role in the nuclear photoabsorption process.

DOI: 10.1103/PhysRevC.73.064607 PACS number(s): 25.20.−x, 25.85.Jg, 24.10.Lx, 24.85.+p

Photon-nucleus reactions are excellent tools for investigating nuclear and nucleonic structures. The photonuclear absorption process, for instance, has been used to study the formation and propagation of baryonic resonances inside nuclear matter [1–6], the photon hadronization process that gives rise to the shadowing effect in the photoabsorption cross section [1,7], or the formation and propagation of hyperons in the nucleus [6]. The simplicity of photonuclear reactions as compared to reactions induced by other probes, from both the theoretical and experimental points of view, is attractive to those willing to study nuclear and subnuclear structures.

However, the various nuclear processes taking place during the reaction, mainly at intermediate and high energies, cause some problems in the comprehension of the nuclear or subnuclear mechanisms. One example is the fissility of heavy nuclei. It was supposed that fissility was an increasing function of the photon energy, and that for actinide nuclei, which present the highest fissility values among the stable nuclei, one could expect their fissility to be 1 for energies above a few hundred MeV [8]. In fact, the measurement of fission cross section was proposed as a reliable method for measuring the total photoabsorption cross section [9,10]. A fine, although incomplete, overview on the theoretical approaches for calculating photofission cross sections is presented in Ref. [11].

Experimental results obtained at Frascati [9,10], Mainz [12,13], Bonn [1,14], Saskatoon [15], and Thomas Jefferson Laboratory [16,17] have shown, however, that this was not the case. The fissility for thorium and several uranium isotopes was found to be lower than that for neptunium, showing that nuclear fissility does not saturate for those nuclei, remaining at a value below 100% even at high incident photon energies. This result was fully explained by a Monte Carlo study of the intranuclear cascade and evaporation/fission competition processes that follows the photon absorption, as implemented by the MCMC and MCEF codes [18,19]. The important feature for explaining the nonsaturation of the heavy-nuclei fissility was the inclusion of protons and α-particles evaporation in the evaporation-fission competition process that follows the intranuclear cascade. Afterwards, the MCMC and MCEF codes were coupled to give the CRISP code, which since has been used to calculate photoabsorption and/or photofission cross sections for several nuclei with mass numbers ranging from 12 up to 238, and for photons of energies from 40 MeV up to 1 GeV, covering the entire range of baryonic resonances [20]. Moreover, an alternative, semiempirical approach has been developed to analyze photofission data in the 0.2–4 GeV region for a number of target nuclei [21,22], where new features of the intranuclear cascade process are discussed. These calculations have shown good agreement with the experimental results. Subsequently, the CRISP model has been applied to proton-nucleus interactions at energies between 200 MeV and 1.2 GeV [23–25], and different observables, such as neutron multiplicities and spallation products distributions, have been evaluated, showing again good results as compared to experimental data. With the inclusion of electron scattering, the CRISP approach has been used also for studying the quasifree electrofission cross section on ^{238}U [26,27].

The CLAS photofission data [16,17], however, extend well above the 1-GeV incident energy region, going up to 3.5 GeV. In this region the photoabsorption process is completely different: the photon has a hadronic component in its wave function and, according to the vector dominance models (VDM), this component presents a cross section considerably higher for interacting with the nucleons. It is the vector meson (hadronic state of the photon) absorption that will initiate the intranuclear cascade.

In Ref. [11] the authors present results on photofission obtained with the RELDIS code for photon energies up to 3.5 GeV. Their results for fissility of uranium isotopes are in qualitative good agreement with experimental data but deviates systematically from the experimental values. For thorium and lead, however, the qualitative agreement is lost, and the calculated fissility as a function of the incident photon energy presents a behavior rather different from that shown by experimental results.

The CRISP code [18–20] has been applied for photon energies from 40 MeV up to 1 GeV, presenting results in good agreement with experimetal data. To extend the CRISP code to higher energies, the hadronization process have been included in the Monte Carlo model. This inclusion follows the VDM. The photon hadronic state is described as a plane wave, and its interaction with nucleons is calculated in first born approximation. This plane wave attenuates while propagating inside the nucleus. The attenuation is because of the interaction of the photon electromagnetic and hadronic fields with the nuclear field. The process can be viewed schematically in Fig. 1. A consequence from the meson dominance in the photoabsorption is the so-called shadowing effect, which shows up in the photoabsorption cross section dependence of the nuclear mass number. In fact, although this dependence

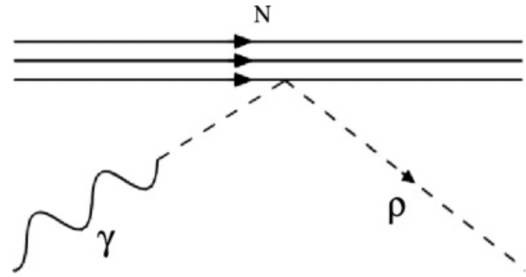

FIG. 1. Schematic representation of the photon-nucleus interaction through the hadronization mechanism.

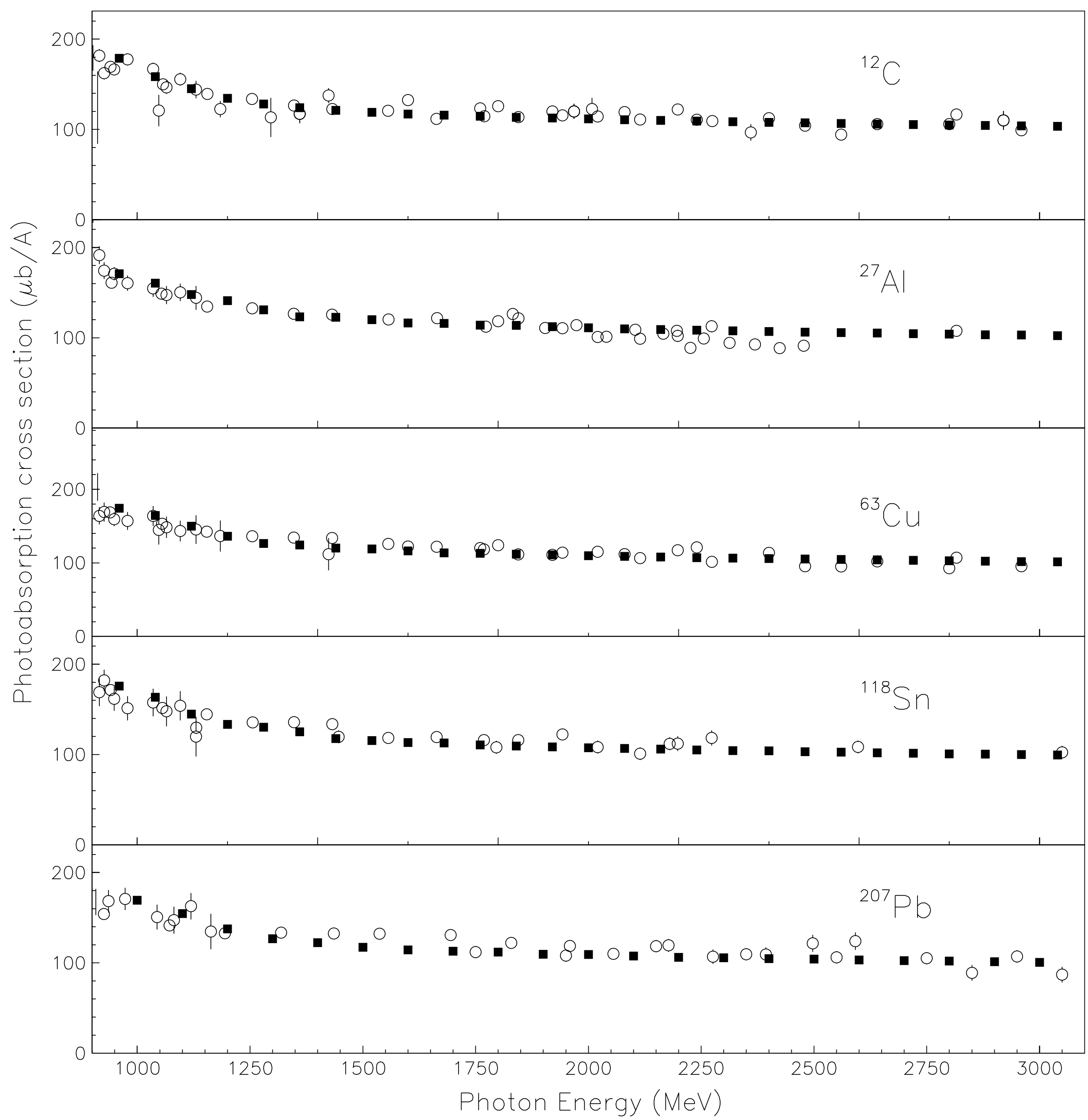

FIG. 2. Total photoabsorption cross section per nucleon for various nuclei. Full squares are the results obtained with the CRISP code (this work); experimental data (open symbols) are taken from Refs. [1,14].

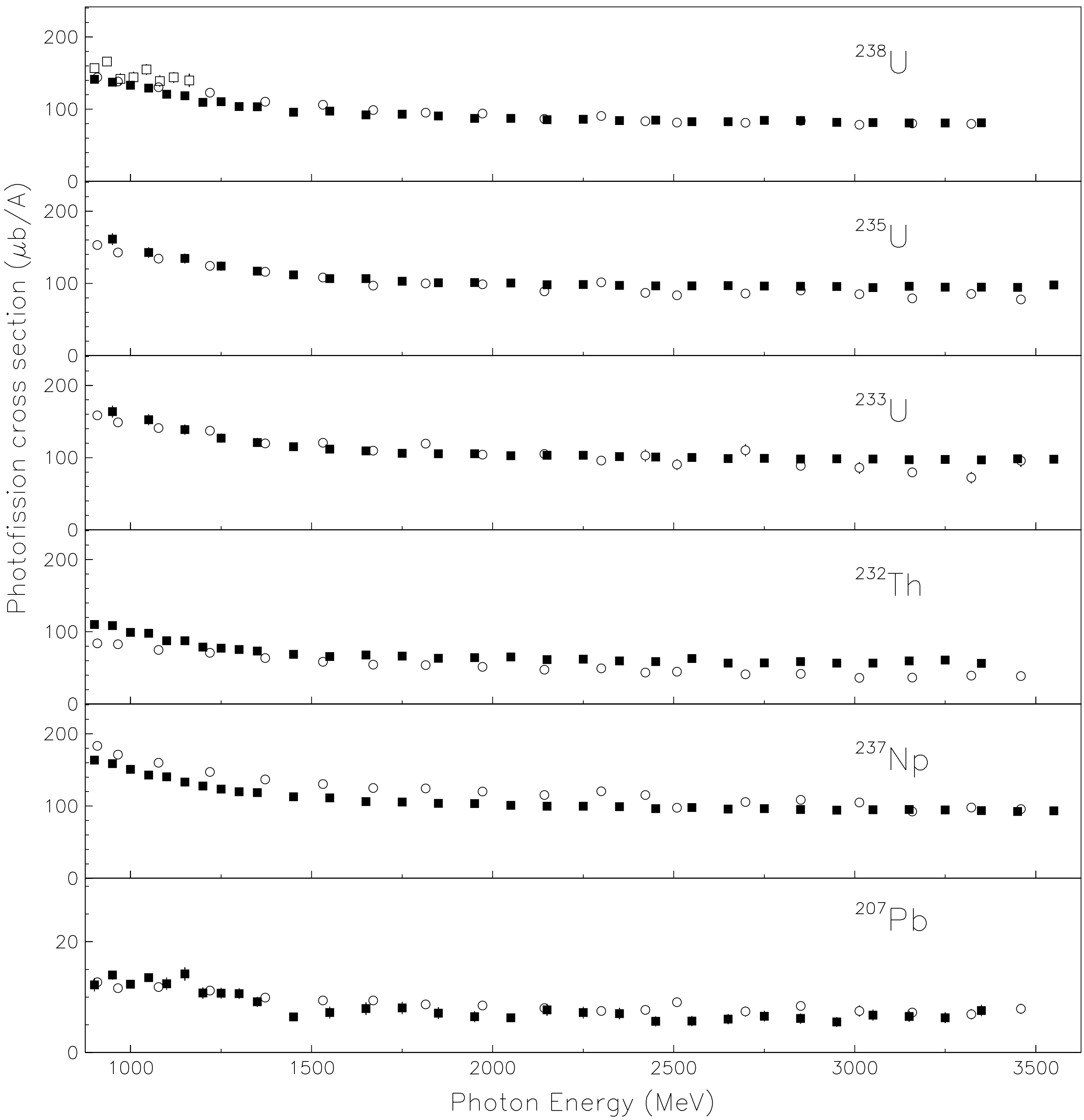

FIG. 3. Photofission cross section per nucleon for various target nuclei. Full squares are the results obtained with the CRISP code (this work); experimental data (open symbols) are taken from Refs. [16,17].

is directly proportional to the mass number below the onset of the shadowing effect, for energies above this threshold the cross section is proportional to A^{α}, where $\alpha \approx 0.9$, according to the experimental results.

The total photoabsorption cross sections normalized by the nuclear mass number for different nuclei from $A = 12$ up to $A = 207$ are shown in Fig. 2 and compared with experimental data available in the literature. We observe a good agreement between calculations with the CRISP code and the experimental results in the entire energy range considered, and for all target nuclei as well.

These results represent strong evidence that the shadowing effect arizing from the photon hadronization process in the presence of nuclear matter is correctly simulated in our code. This effect depends on the nucleon Fermi motion, the cross section for the interaction between the produced vector-meson and the nucleons, and the nuclear density, among other physical quantities.

The photofission cross section calculated with the CRISP code for different heavy nuclei at the shadowing effect region is presented in Fig. 3 and compared with experimental results, showing again good agreement with the experiments for all nuclei and in the entire energy range studied.

The good agreement with experimental data indicates that the cascade and evaporation/fission processes are correctly calculated by the CRISP model, confirming previous results obtained for these and other nuclei at the quasideuteron and baryon-resonances regions [20]. It is important to remark that all parameters in the CRISP code used in the present work have the same values as those used in [20,23–27]. Therefore, with only one set of parameters, the CRISP model is able reproduce experimental results for a variety of observables in nuclei from carbon to uranium, and at an energy range from 40 MeV up to 3.5 GeV, and for different probes such as photons, electrons, and protons. These results could be obtained because a correct simulation of the many different processes during the nuclear reactions has been performed. In the case of the present work, although the results for photoabsorption cross section show that the primary interaction via the photon-hadronization process is correctly performed in our Monte Carlo code, the photofission results show that the intranuclear cascade process initiated by the vector-meson absorption is correctly simulated with the same methods used at lower energies.

Because experimental data on total photoabsorption cross sections for actinide nuclei are not yet available, we do not plot the results obtained with the CRISP code for those quantities. However, the cross section for actinides show the same smooth behavior of the cross section for the lighter nuclei presented in this work. The only target for which we have experimental data for both photofission and total photoabsorption cross sections is ^{207}Pb. We observe in Figs. 2 and 3 that both cross sections are correctly calculated by the CRISP code. Therefore, we may conclude that fissility is also correctly calculated for this nucleus. The same conclusion we can extend to actinide nuclei, because of the similar results obtained for the photoabsorption cross section, as it is expected to be according the VDM model.

We notice that the calculated results in Fig. 3 for Np are systematically below the experimental data. As already observed in Ref. [20], the photofission cross section for neptunium is above the so-called universal curve for total photoabsorption cross section. Thus, one has to suppose fissility higher than 100% to reproduce the photofission experimental data. Two possible explanations for this result are (a) the total photoabsorption cross section for neptunium is higher than the universal curve assumed for all other nuclei or (b) there is an experimental error, possibly in the evaluation of the neptunium target mass, resulting in systematic deviation of the measured cross section.

For thorium the calculated photofission cross section is systematically above the experimental data in the energy range considered in this work (Fig. 3). As shown in Ref. [20], this behavior is not observed for energies below 1 GeV. As the energy increases, the residual nuclei formed at the end of the intranuclear cascade have smaller mass numbers and, thus, they have different values for the fission barrier and for the level-density parameter as well. Nuclear fissility is strongly dependent on these quantities, and small errors in their parametrization can induce large deviations in the photofission cross section. The small deviations observed for thorium in Fig. 3 can be attributed to errors in the calculation of fission barrier or level-density parameter. We are currently working on improvements of these calculations, and toward this end we have to take into account also other reactions, such as spallation induced by photons and by protons. A detailed description on this subject will be presented in the near future.

In the case of lead, we observe fluctuations in the photofission cross section which are the result of somewhat poor statistics. The fissility for this nucleus is around 7%, considerably smaller than that for actinides. However, we do not exclude possible physical oscillations in fissility, because it results from a complex combination of fission probabilities for all different nuclides formed during the evaporation process.

Comparing the results obtained in this work with those obtained by the RELDIS code [11], we observe a better agreement with experimental data for the first ones, although the RELDIS model presents an approach to the evaporation-fission competition process that is in many aspects similar to that of the CRISP code. A possible explanation can be the significant differences in the approach to the intranuclear cascade process. In the CRISP method, the collisions among nucleons and mesons are followed in a time-ordered sequence, as introduced in Ref. [28], contrarily to the approach used in the RELDIS code. As discussed in Ref. [20], the CRISP code allows for a more realistic simulation of the reaction mechanisms during the cascade, such as Pauli blocking or density fluctuations. Also, some physical aspects can be more firmly determined as, for instance, the end of the intranuclear cascade process and the occupation numbers for nucleonic levels in the residual nucleus.

[1] V. Muccifora *et al.*, Phys. Rev. C **60**, 064616 (1999).
[2] M. Anghinolfi *et al.*, Phys. Rev. C **47**, R922 (1993).
[3] M. Anghinolfi *et al.*, Nucl. Phys. **A553**, C631 (1993).
[4] N. Bianchi *et al.*, Phys. Lett. **B309**, 5 (1993).
[5] M. Gonçalves *et al.*, Phys. Lett. **B406**, 1 (1997).
[6] M. Gonçalves *et al.*, Braz. J. Phys. **34(3A)**, 919 (2004).
[7] N. Bianchi, E. De Sanctis, M. Mirazita, and V. Muccifora, Phys. Rev. C **60**, 064617 (1999).
[8] J. Ahrens *et al.*, Phys. Lett. **B146**, 303 (1984).
[9] N. Bianchi *et al.*, Phys. Rev. C **48**, 1785 (1993).
[10] N. Bianchi *et al.*, Phys. Lett. **B299**, 219 (1993).
[11] I. A. Pshenichnov *et al.*, Eur. Phys. J. A **24**, 69 (2005).
[12] T. Frommhold *et al.*, Phys. Lett. **B295**, 28 (1992).
[13] T. Frommhold *et al.*, Z. Phys. A **350**, 249 (1994).
[14] M. Mirazita *et al.*, Phys. Lett. **B407**, 225 (1997).
[15] J. C. Sanabria *et al.*, Phys. Rev. C **61**, 034604 (2000).
[16] C. Cetina *et al.*, Phys. Rev. Lett. **84**, 5740 (2000).
[17] C. Cetina *et al.*, Phys. Rev. C **65**, 044622 (2002).
[18] A. Deppman, O. A. P. Tavares, S. B. Duarte, E. C. deOliveira, J. D. T. Arruda-Neto, S. R. dePina, V. P. Likhachev,

O. Rodriguez, J. Mesa, and M. Goncalves, Phys. Rev. Lett. **87**, 182701 (2001).

[19] A. Deppman, O. A. P. Tavares, S. B. Duarte, J. D. T. Arruda-Neto, M. Goncalves, V. P. Likhachev, and E. C. deOliveira, Phys. Rev. C **66**, 067601 (2002).

[20] A. Deppman *et al*., J. Phys. G: Nucl. Part. Phys. **30**, 1991 (2004).

[21] O. A. P. Tavares *et al*., J. Phys. G: Nucl. Part. Phys. **30**, 377 (2004).

[22] O. A. P. Tavares *et al*., Braz. J. Phys. **35(3B)**, 915 (2005).

[23] S. Anefalos *et al*., Nucl. Sci. Eng. **151**, 82 (2005).

[24] S. Anefalos *et al*., Braz. J. Phys. **34(3A)**, 966 (2004).

[25] S. Anefalos *et al*., Braz. J. Phys. **35(3B)**, 912 (2005).

[26] V. P. Likhachev *et al*., Phys. Rev. C **68**, 014615 (2003).

[27] V. P. Likhachev *et al*., Nucl. Phys. **A713**, 24 (2003).

[28] T. Kodama, S. B. Duarte, K. C. Chung, and R. A. M. S. Nazareth, Phys. Rev. Lett. **49**, 536 (1982).